# High-Momentum Protons in $^{208}$Pb

I. Bobeldijk, M. Bouwhuis, D. G. Ireland,* C. W. de Jager, E. Jans, N. de Jonge, W-J. Kasdorp, J. Konijn, L. Lapikás, J. J. van Leeuwe, R. L. J. van der Meer, G. J. L. Nooren, E. Passchier, M. Schroevers, G. van der Steenhoven, J. J. M. Steijger, J. A. P. Theunissen, M. A. van Uden, H. de Vries, R. de Vries, and P. K. A. de Witt Huberts

*National Institute for Nuclear Physics and High-Energy Physics (NIKHEF, section K), P.O. Box 41882, 1009 DB Amsterdam, The Netherlands*

H. P. Blok, H. B. van den Brink, G. E. Dodge, M. N. Harakeh,† W. H. A. Hesselink, N. Kalantar-Nayestanaki,† A. Pellegrino, C. M. Spaltro, and J. A. Templon

*Department of Physics and Astronomy, Vrije Universiteit, De Boelelaan 1081, 1081 HV Amsterdam, The Netherlands*

R. S. Hicks

*Department of Physics, University of Massachusetts, Amherst, Massachusetts 01003*

J. J. Kelly

*Department of Physics, University of Maryland, College Park, Maryland 20742*

C. Marchand

*Centre d'Etudes Nucléaires de Saclay, Departement d'Astrophysique, Physique des Particules, Physique Nucleare et d'Instrumentation Assocciee/Service de Physique, F-91191, Gif-sur-Yvette, France*

(Received 19 July 1994)

High-momentum components of proton momentum distributions in $^{208}$Pb have been studied from 300 to 500 MeV/$c$ with the $(e, e'p)$ reaction. Cross sections were measured with 180 keV excitation-energy resolution for transitions to the low-lying $\frac{1}{2}^+$, $\frac{3}{2}^+$, $\frac{11}{2}^-$, $\frac{5}{2}^+$, and $\frac{7}{2}^+$ states in $^{207}$Tl. The data are compared to distorted-wave impulse-approximation calculations with mean-field wave functions and with wave functions that include nucleon-nucleon correlations. The data are substantially larger than mean-field predictions. The observed excess strength at low excitation energy appears to be mainly due to long-range correlations and not to short-range and tensor correlations.

PACS numbers: 25.30.Fj, 27.80.+w

The atomic nucleus is a many-body quantum system, in which correlations between the constituent nucleons play an important role. In proton knockout experiments [1–3] with the reaction $(e, e'p)$, it has been observed that correlations cause the spectroscopic strength for a single-particle orbit to be quenched with respect to uncorrelated mean-field values and fragmented over a large excitation energy domain in the spectral function. Moreover, the correlations are related to the momentum dependence of the spectral function. In particular, short-range (SRC) and tensor correlations (TC) will have a large effect on nucleons at short mutual distances. Therefore, such correlations will affect the single-nucleon wave function predominantly in the nuclear interior, corresponding to a modification of the high-momentum part in its Fourier transform, the single-nucleon momentum distribution.

Conflicting predictions for the strength of the induced high-momentum components exist. With a self-consistent Green's function method, Müther and Dickhoff [4] have explicitly included SRC in the calculation of the $^{16}$O momentum distribution. They observed no significant increase at high momentum and low excitation energy compared to a mean-field result. Rather, the high-momentum part of the momentum distribution increases significantly at excitation energies larger than about 50 MeV. Similar observations have been made in calculations for correlated infinite nuclear matter [5,6]. For finite nuclei Pandharipande *et al.* [7,8] obtained quasiparticle wave functions which include the effects of SRC by applying the results of variational Monte Carlo calculations of correlated quantum drops of liquid $^3$He to the nuclear system. In the latter technique long-range correlations are not accounted for.

In contrast, other authors predict an enhanced probability of the high-momentum components for transitions at low excitation energy. Ma and Wambach [9,10] and Mahaux *et al.* [11,12] employed an effective mass for the nucleon in the nuclear medium to account for the effect of correlations. In their approach, the quasiparticle wave functions are not only suppressed in the nuclear interior but also enhanced at the nuclear surface due to long-range correlations.

The various calculations predict high-momentum components that differ by 1 to 2 orders of magnitude in the range from 300 to 500 MeV/$c$. An $(e, e'p)$ experiment in this domain suffers from low count rate and was thus far impossible due to the poor real-to-accidental ratio at the required luminosity. With the high-duty factor facility

 0031-9007/94/73(20)/2684(4)$06.00 

AmPS at NIKHEF-K a $^{208}$Pb$(e, e'p)$ experiment has been performed with adequate real-to-accidental ratios. The nucleus $^{208}$Pb was chosen as target because momentum distributions for transitions to final states with different quantum numbers can be determined. Hence one samples the proton wave functions at different average densities. In this Letter we report on this experiment and compare the data to distorted-wave impulse-approximation calculations with mean-field wave functions and wave functions that include the effects of nucleon-nucleon correlations.

The experiment was carried out with the electron beam from the Amsterdam Pulse-Stretcher facility (AmPS) at NIKHEF-K [13] at an energy of 487.3 ± 0.5 MeV. The duty factor and the average current of the beam amounted to about 50% and 1.5 $\mu$A, respectively. The scattered electron and knocked-out proton were detected in coincidence by two high-resolution magnetic spectrometers [14].

The present data between 300 and 500 MeV/$c$ were measured under kinematical conditions where the center of the acceptance corresponded to fixed values of the three-momentum transfer ($q$ = 221 MeV/$c$), the energy transfer ($\omega$ = 110 MeV), and the proton kinetic energy ($T_{p'}$ = 100 MeV, corresponding to a proton momentum of $p'$ = 444.6 MeV/$c$). The angle of the proton spectrometer was set at 99.17°, 112.18°, and 139.11° to obtain a missing momentum of 340, 400, and 500 MeV/$c$ in the center of the acceptance, respectively. At each setting the covered missing momentum range is ±30 MeV/$c$. The experimental quantity missing momentum is defined as $\mathbf{p}_m = \mathbf{p}' - \mathbf{q}$ and can, in the plane-wave impulse approximation, be identified with the initial momentum of the ejected proton. For brevity we will refer to $p_m$ as momentum.

The target consisted of two enriched (abundancy 99%) $^{208}$Pb foils separated by 5 mm and mounted in a water-cooled frame. With the double-foil construction the luminosity could be doubled while maintaining the excitation-energy resolution at 180 keV by separating the events from the foils through vertex reconstruction and subsequently accounting for position dependent energy loss in the target. The total target thickness of 87.4 ± 2.8 mg/cm$^2$ has been determined by comparing the measured cross section for elastic electron scattering with the calculated cross section from known Fourier-Bessel coefficients [15]. The total systematic uncertainty in the cross sections is 6%.

As a check of the performance of the total experimental system a calibration run was made on $^{208}$Pb at $p_m$ = 150 MeV/$c$ and a proton kinetic energy of 100 MeV in parallel kinematics. Quint [16] has determined the cross section under these conditions with an accuracy of 3%. Our data reproduced this measurement within the statistical error of 8%. During the experiment, calibration runs were carried out regularly at $p_m$ = 220 MeV/$c$ to monitor the beam energy and the overall normalization.

In Fig. 1 the reduced cross section, which is defined as the sixfold differential cross section divided by the off-shell electron-proton cross section $\sigma_{cc1}^{ep}$ as given by De Forest [17] and by the appropriate kinematical factor, is displayed at a mean momentum of 340 MeV/$c$. Accidental coincidences have been subtracted, the phase space has been accounted for, and the spectrum has been unfolded for radiative processes [18]. The peaks in this excitation-energy spectrum are well separated. From the reduced cross section, momentum distributions have been obtained by integrating the individual peaks. At a momentum of 500 MeV/$c$ only an upper limit of the momentum distribution has been obtained due to low statistics.

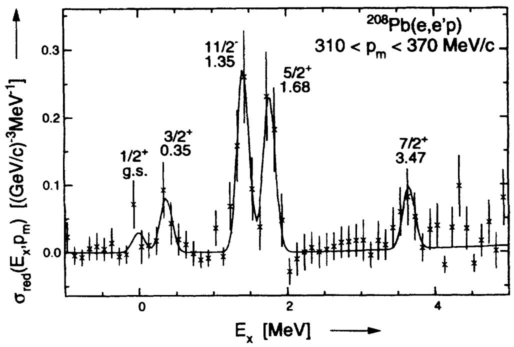


FIG. 1. The reduced cross section of the reaction $^{208}$Pb$(e, e'p)$ at an average missing momentum of 340 MeV/$c$, showing the knock out of valence protons to discrete states in $^{207}$Tl, labeled by their spin, parity, and excitation energy. The solid curve is the result of a fit to the spectrum.

In Fig. 2 the momentum distributions for the transitions to the dominant $\frac{1}{2}^+$, $\frac{3}{2}^+$, $\frac{11}{2}^-$, $\frac{5}{2}^+$, and $\frac{7}{2}^+$ single-hole states in $^{207}$Tl as measured in the present experiment (solid circles) are compared to the data of Quint (plus marks) [16]. The data at low momenta were measured in parallel kinematics, whereas the data at high momentum were obtained in $(q, \omega)$-constant kinematics, where $q$ and $\omega$ are kept constant while changing $p_m$. In order to account for the kinematical dependence of Coulomb distortions in these measurements, the data are plotted as a function of the effective missing momentum $p_m^{\text{eff}}$, which has been employed by Jin *et al.* [19]. This effective missing momentum is defined by $\mathbf{p}_m^{\text{eff}} = \mathbf{p}' - \mathbf{q}^{\text{eff}} = \mathbf{p}' - [\mathbf{k}_f(1 + f_c\alpha Z/R_c k_f) - \mathbf{k}_i(1 + f_c\alpha Z/R_c k_i)]$, with $k_i$ the initial and $k_f$ the final electron momentum, $R_c$ = 7.1 fm and $f_c$ = 1.5.

The solid curves in Fig. 2 are the result of distorted-wave impulse-approximation calculations including electron and proton distortions (CDWIA) [20]. The optical model parameters used in the calculations have been taken from Refs. [21] and [22]. For the bound-state wave functions we used mean-field wave functions $\phi(r)$ generated in a Woods-Saxon potential and normalized to give $\langle\phi(\mathbf{r})|\phi(\mathbf{r})\rangle = 1$. In the present analysis the normalization factors ($N$ = 1.09, 2.27, 6.96, 3.21, and 2.06 for the transitions to the $\frac{1}{2}^+$, $\frac{3}{2}^+$, $\frac{11}{2}^-$, $\frac{5}{2}^+$, and $\frac{7}{2}^+$ states in $^{207}$Tl, respectively) and the radial parameters of the

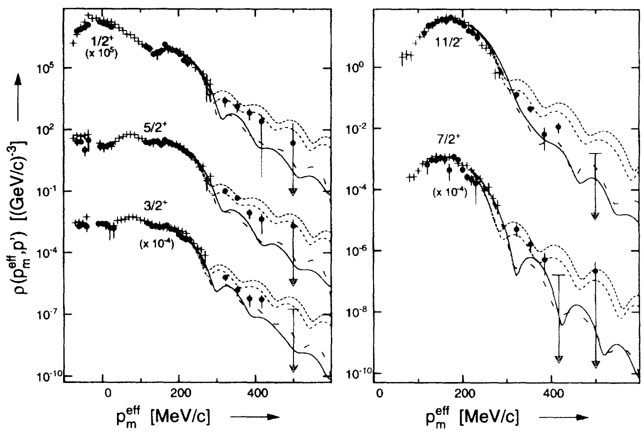

FIG. 2. Missing-momentum distributions for the transitions to the $\frac{1}{2}^+$, $\frac{3}{2}^+$, $\frac{11}{2}^-$, $\frac{5}{2}^+$, and $\frac{7}{2}^+$ states in the reaction $^{208}$Pb$(e, e'p)$ at excitation energies of 0.00, 0.35, 1.35, 1.68, and 3.47 MeV, respectively. The present data are represented by solid circles, the plus marks have been measured by Quint [16]. The solid curves are knockout calculations in the distorted-wave impulse approximation. The calculations including correlations as proposed by Pandharipande [8], Ma and Wambach [10], and Mahaux and Sartor [12] are represented by dash–double-dotted, dashed, and dot-dashed curves, respectively.

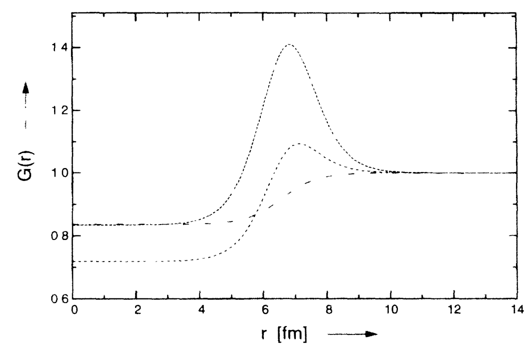

FIG. 3. The function $G(r)$ which is employed to convert mean-field nucleon wave functions in $^{208}$Pb to quasiparticle wave functions, according to the prescriptions of Pandharipande [8] (dash–double-dotted), Ma and Wambach [10] (dashed), and Mahaux and Sartor [12] (dot-dashed).

potential have been determined by fitting CDWIA curves to the data at low momentum. In passing we note that a comparison of these data with full relativistic calculations [19] yields spectroscopic factors that are typically 10%–15% larger than the aforementioned normalization factors $N$. Calculations including correlations as proposed by Pandharipande *et al.* [8], Ma and Wambach [10], and Mahaux and Sartor [12] are represented by dash–double-dotted, dashed, and dot-dashed curves, respectively. The latter three curves result from CDWIA calculations employing quasiparticle wave functions $\Phi^\star(r)$ and the same normalization factors $N$ as given above. We have constructed these $\Phi^\star(r)$ by converting the mean-field wave functions $\phi(r)$ by the relation $\Phi(r) = G(r)\phi(r)$, where $G(r)$ is shown in Fig. 3 for $^{208}$Pb. The resulting quasiparticle wave functions were renormalized via $\Phi^\star(r) = \Phi(r)/\sqrt{R}$ to give $\langle\Phi^\star(\mathbf{r})|\Phi^\star(\mathbf{r})\rangle = 1$. The renormalization factors $R$ for the five transitions are in the range {0.75–0.79}, {0.72–0.83}, and {1.15–1.34} for the quasiparticle wave functions according to Pandharipande, Mahaux and Sartor, and Ma and Wambach, respectively.

The appreciable difference in shape between the conversion function $G(r)$ of Pandharipande relative to that of Ma and Wambach and Mahaux and Sartor is due to the presence of long-range correlations in the latter calculations. Ma and Wambach and Mahaux and Sartor use phenomenological models of the quasiparticle effective mass, which is the product of two terms: the $k$ mass, which is determined by the momentum dependence of the self-energy, and the $E$ mass, which is determined by its energy dependence. Suppression of the $k$ mass below unity is attributed to short-range correlations arising from the nucleon-nucleon interaction and the exchange contribution to the Hartree-Fock potential. Long-range correlations are included via the coupling of the hole state to low-lying excitations, which leads to an enhancement of the $E$ mass, particularly at the surface.

In order to compare to the data, the calculated CDWIA cross sections are divided by the electron-proton cross section of McVoy-Van Hove $\sigma_{\rm NR}^{ep}$ [23] and by the appropriate kinematical factor. In this way we account for the fact that the nucleon-current operator that is used in the CDWIA calculation is a nonrelativistic expansion of the one that is used in $\sigma_{cc1}^{ep}$. The ratio of $\sigma_{\rm NR}^{ep}/\sigma_{cc1}^{ep}$ varies from 1.2 to 1.7 over the covered momentum range. In order to account for eikonal approximations made in the treatment of electron distortions in CDWIA as compared to the full relativistic calculation of Jin *et al.* [19], we have plotted the CDWIA curves against $p_m^{\rm eff}$ with $f_c = 2.0$.

The curves that include correlations according to the Pandharipande prescription do not significantly differ from the mean-field calculations, indicating that within the above discussed approach the effect of short-range and tensor correlations is small in the presently investigated domain of momentum and energy. A similar observation was made by Müther and Dickhoff [4]. In contrast, the calculations of Ma and Wambach and Mahaux and Sartor differ significantly from the mean-field calculations. Clearly, long-range correlations—which are only included in the calculations of Ma and Wambach and Mahaux—have a large effect on the shape of the quasiparticle wave functions. As a result, the momentum distributions are appreciably enhanced at high momenta.

The high-momentum data are substantially larger than the mean-field momentum distributions and the curves including the SRC and TC as prescribed by Pandharipande. Rather, the data tend to prefer the momentum distributions calculated from quasiparticle wave functions given by Mahaux and Sartor and Ma and Wambach. This preference is an indication of the importance of long-range correlations. Furthermore, we observe that the experimental data for transitions to final states with different quantum numbers all show a similar behavior. In particular, no significant difference is seen for knock out from the surface-peaked $1h_{\frac{11}{2}}$ and $1g_{\frac{7}{2}}$ orbitals and those from the multinodal $3s_{\frac{1}{2}}$, $2d_{\frac{3}{2}}$, and $2d_{\frac{5}{2}}$ orbitals. The latter momentum distributions receive appreciable strength from the interior part of the wave functions. Hence, we have no indication for a density dependence of the observed high-momentum components.

By integrating the momentum distributions according to Mahaux and Sartor, which roughly reproduce the data, we find that the number of protons associated with the data in the momentum range of $\{300–500\ \mathrm{MeV}/c\}$ is <0.5% of the corresponding number of protons in the momentum range $\{0–300\ \mathrm{MeV}/c\}$. This implies that a considerable part of the unobserved protons should be located at higher excitation energy as suggested by Ref. [4] for $^{16}$O and Refs. [5] and [6] for nuclear matter.

Thus far the data have been interpreted in the framework of a one-body current operator. Going beyond this approach, meson-exchange currents (MEC) could be considered. Their influence is estimated to be small as the present data have been collected in dominantly longitudinal kinematics ($\epsilon = 0.87$), although MEC may contribute to the cross section via the longitudinal-transverse interference structure function $W_{LT}$. Boffi and Radici investigated the contribution of MEC and isobar configurations in the reaction $^{40}\mathrm{Ca}(e, e'p)^{39}\mathrm{K}$ in comparable $(q, \omega)$-constant kinematics and concluded their effect to be about 10% of the one-body contribution at high momenta [24].

In summary, an electron-induced proton knockout experiment on $^{208}$Pb has been carried out in $(q, \omega)$-constant kinematics covering the momentum range between 300 and 500 MeV/$c$. The data have been compared to CDWIA calculations with mean-field wave functions and with quasiparticle wave functions. For final states at low excitation energy the effect of short-range and tensor correlations on the observed strength at high momentum is less important than that of long-range correlations. No significant differences have been observed in the high-momentum behavior of $3s_{\frac{1}{2}}$, $2d_{\frac{3}{2}}$, $1h_{\frac{11}{2}}$, $2d_{\frac{5}{2}}$, and $1g_{\frac{7}{2}}$ proton knock out. Since the calculations of Ref. [4] indicate that the effects of short-range and tensor correlations increase with excitation energy, further work should be devoted to measurements of high-momentum components at large excitation energies.

We would like to thank all technicians and physicists who made this difficult first experiment with AmPS a success. We are grateful to I. Sick for his suggestion to use the multifoil target technique and to V. Pandharipande for his comments on quasiparticle wave functions. This work is part of the research program of the Foundation for Fundamental Research of Matter (FOM), which is financially supported by the Netherlands' Organisation for Advancement of Pure Research (NWO).

*Present address: Department of Physics & Astronomy, University of Glasgow, Glasgow G12 8QQ, United Kingdom.

†Present address: KVI, Zernikelaan 25, 9747 AA Groningen, The Netherlands.

[1] L. Lapikás, Nucl. Phys. **A553**, 297c (1993).
[2] P. K. A. de Witt Huberts, J. Phys. G **16**, 507 (1990).
[3] G. van der Steenhoven, Nucl. Phys. **A527**, 17c (1991).
[4] H. Müther and W. H. Dickhoff, Phys. Rev. C **49**, R17 (1994).
[5] O. Benhar, A. Fabrocini, and S. Fantoni, Nucl. Phys. **A505**, 267 (1989).
[6] A. Ramos, A. Polls, and W. H. Dickhoff, Nucl. Phys. **A503**, 1 (1989); B. E. Vonderfecht, W. H. Dickhoff, A. Polls, and A. Ramos, Nucl. Phys. **A555**, 1 (1993).
[7] V. R. Pandharipande *et al.*, Phys. Rev. Lett. **53**, 1133 (1984).
[8] V. R. Pandharipande and S. C. Pieper, Nucl. Phys. **A507**, 167c (1990); (private communication).
[9] Z. Y. Ma and J. Wambach, Nucl. Phys. **A402**, 402 (1983).
[10] Z. Y. Ma and J. Wambach, Phys. Lett. **B 256**, 1 (1991).
[11] C. Mahaux and H. Ngo, Nucl. Phys. **A431**, 486 (1984).
[12] C. Mahaux and R. Sartor, Adv. Nucl. Phys. **20**, 1 (1991).
[13] P. K. A. de Witt Huberts, Nucl. Phys. **A553**, 845c (1993).
[14] C. de Vries *et al.*, Nucl. Instrum. Methods **223**, 1 (1984).
[15] H. de Vries, C. W. de Jager, and C. de Vries, At. Data Nucl. Data Tables **36**, 495 (1987).
[16] E. N. M. Quint, Ph.D. thesis, University of Amsterdam, 1988 (unpublished).
[17] T. de Forest, Jr., Nucl. Phys. **A392**, 232 (1983).
[18] J. W. A. den Herder *et al.*, Nucl. Phys. **A490**, 507 (1988).
[19] Y. Jin, H. P. Blok, and L. Lapikás, Phys. Rev. C **48**, R964 (1993).
[20] C. Giusti and F. Pacati, Nucl. Phys. **A485**, 461 (1988).
[21] J. Raynal, Report No. IAEA-SMR-918, 1972 (to be published).
[22] H. P. Blok, L. R. Kouw, J. W. A. den Herder, L. Lapikás, and P. K. A. de Witt Huberts, Phys. Lett. **B 198**, 4 (1987).
[23] H. P. Blok, in Proceedings of the International Conference, Trieste, 1993 (unpublished).
[24] S. Boffi and M. Radici, Phys. Lett. **B 242**, 151 (1990); (private communication).